Wavelet Based Multigrid Reconstruction Algorithm for Optical Tomography

Wenwu Zhu*, Yao Wang*, Yuqi Yao*, and Randall L. Barbour†

*Department of Electrical Engineering
Polytechnic University, Brooklyn, NY 11201

†Departments of Pathology and Biophysics
SUNY Health Science Center, Brooklyn, NY 11203

Abstract

In this paper, we present a wavelet based multigrid approach to solve the perturbation equation encountered in optical tomography. The wavelet based multigrid representation has been applied to obtain regularized least squares (RLS) and total least squares (TLS) solutions. The unknown image, the data, as well as the weight matrix are all represented by wavelet expansions, thus yielding a multiresolution representation of the perturbation equation. Then, the transformed perturbation equation is solved by either the RLS or TLS method, using a multigrid scheme, by which an increasing portion of wavelet coefficients of the unknown image are solved in successive approximations. The experimental results show that the multigrid method can achieve similar reconstruction quality with a significantly reduced amount of time than the one-grid algorithm.

Key Words

Image Reconstruction, Wavelets, Tomographic Imaging, and Optical Imaging.

Introduction

In this paper, we consider the recovery of optical properties in scattering media from continuous wave (CW) near infrared optical measurements. The problem is difficult because in this frequency range, photons propagate through the tissue in a highly diffused manner and the relation between the measured signal and the absorption properties of the media is non-linear. In the past few years, our group has developed an iterative perturbation approach for both CW, TR [1-2] and frequency domain data [3]. This requires the solution of a linear perturbation equation at each iteration:

$$\mathbf{Hx} = \mathbf{y}, \tag{1}$$

where $\mathbf{x}$ is an $N \times 1$ vector of differences in the absorption properties between a reference and test medium, $\mathbf{y}$ is an $M \times 1$ vector of changes in detector readings between the two media, and $\mathbf{H}$ is an $M \times N$ matrix of weights describing the influence of each volume element (voxel) on the detector readings, which are essentially the derivatives of the detector readings with respect to the absorption coefficients in the reference medium. In general, the perturbation equation is both underdetermined and ill-posed. To solve the linear perturbation equation, several iterative algorithms have been developed, including projection onto convex sets (POCS) [1], CGD [1], multigrid reconstruction [1], layer stripping [2,4] (for TR data), regularized least squares (RLS) [4], and total least squares (TLS) [5].

One challenging problem in solving the perturbation equation is that the computation complexity is usually very high due to the extremely large dimension of the weight matrix. In order to reduce the computation time, a wavelet based reconstruction algorithm is investigated in this paper. The unknown, the data and the weight matrix are expanded using wavelet, thus yielding a multi-resolution representation of the perturbation equation and the Rayleigh quotient function in wavelet domain. The transformed perturbation equation and the Rayleigh quotient function are solved from coarse to fine resolutions using the solution obtained from the previous resolution as the initial solution in the present resolution. The computational complexity is reduced significantly, compared to a one grid method which solves the equation in the finest resolution directly.

OSA TOPS on Advances in Optical Imaging and Photon Migration
1996, Vol. 2, R. R. Alfano and James G. Fujimoto (eds.)

Multi-Resolution Representation of the Problem

Wavelet Transform as a Multi-resolution Representation

Wavelet transform, as any other linear transform, represents a signal as a linear combination of some basis signals. Here, we give an intuitive interpretation of the wavelet transform, without invoking the quite complicated mathematical description. The basis signals in a wavelet transform are formed by dilating (i.e. scaling) and translating some prototype functions known as scaling and wavelet functions. In an orthogonal wavelet transform, these functions and the scaling and translation parameters are chosen so that the resulting basis signals form an orthonormal set, and the coefficients are simply obtained by the inner product of the signal with the basis signals. By properly chosing the translation and scaling factors, the coefficients can form a multiresolution representation of the original signal. For example, for a two level representation of a discrete one dimensional signal, one group of the basis signals is derived from a scaling function (e.g. with a Gaussian like shape) by translations at two sample intervals. The coefficients associated with these bases form a coarse resolution representation (with half number of samples) of the original signal. The other group is derived from a wavelet function (e.g. with a Laplacian of Gaussian like shape), also by translation at two sample intervals. The coefficients associated with this group represent the details of the signal. These two groups of coefficients are also referred to as the low-frequency and high frequency subsignals, respectively. The low-frequency subsignal can be further decomposed into low and high frequency subsignals, to form a three level representation.

Let $\mathbf{x}$ represent the original signal in a vector form, and let $\mathbf{W}^T$ represent the matrix containing the basis vectors, which satisfies $\mathbf{W}^T\mathbf{W} = \mathbf{W}\mathbf{W}^T = \mathbf{I}$. Then the transformed signal is obtained by

$$\tilde{\mathbf{x}} = \mathbf{W}\mathbf{x} = \begin{bmatrix} \tilde{\mathbf{x}}_l \\ \tilde{\mathbf{x}}_h \end{bmatrix}, \tag{2}$$

where $\tilde{\mathbf{x}}_l$ and $\tilde{\mathbf{x}}_h$ are the low and high frequency subsignals, respectively. The original signal can be recovered from the transformed signal by:

$$\mathbf{x} = \mathbf{W}^T\tilde{\mathbf{x}}. \tag{3}$$

For a two dimensional signal, the wavelet transform can be applied sequentially to the rows and columns. In a two level representation, the size of the coarse resolution subsignal will be a quarter of the original, containing low frequency components in both horizontal and vertical directions. There will be three detail subsignals, containing the low-high, high-low, and high-high frequency contents, respectively. Here, the term low-high, for example, means low frequency in the horizontal direction and high frequency in the vertical direction.

The Perturbation Equation in the Wavelet Domain

Let the transform matrices for $\mathbf{x}$ and $\mathbf{y}$ be represented by $\mathbf{W_x}$ and $\mathbf{W_y}$, respectively. We assume both matrices are orthonormal. Multiplying Eq. (1) from left by $\mathbf{W_y}$ and inserting $\mathbf{W_x}^T\mathbf{W_x} = \mathbf{I}$ in between $\mathbf{H}$ and $\mathbf{x}$, we obtain:

$$\tilde{\mathbf{H}}\,\tilde{\mathbf{x}} = \tilde{\mathbf{y}}, \tag{4}$$

where $\tilde{\mathbf{x}} = \mathbf{W_x}\mathbf{x}$, $\tilde{\mathbf{y}} = \mathbf{W_y}\mathbf{y}$, and $\tilde{\mathbf{H}} = \mathbf{W_y}\mathbf{H}\mathbf{W_x}^T$. Eq. (4) is the perturbation equation in the wavelet domain. From this equation, one can solve $\tilde{\mathbf{x}}$, and then obtain $\mathbf{x}$ by an inverse transform $\mathbf{x} = \mathbf{W_x}^T\,\tilde{\mathbf{x}}$.

Multiresolution Representation of RLS

Regularization is a well-established technique for dealing with instability in inverse problems and can convert an ill-posed problem into a well-posed problem by incorporating *a priori* knowledge about the image to be recovered. Regularized least squares (RLS) can be formulated as

$$\hat{\mathbf{x}} = \arg\min_{\mathbf{x}}\{\|\mathbf{H}\mathbf{x} - \mathbf{y}\|^2 + \lambda\|\mathbf{x}\|^2\}, \tag{5}$$

where the *regularization parameter* λ can be determined by the Miller criterion or Cross-validation method [4]. The RLS solution is given by

$$\hat{\mathbf{x}} = (\mathbf{H}^T\mathbf{H} + \lambda\mathbf{I})^{-1}\mathbf{H}^T\mathbf{y}. \tag{6}$$

In the wavelet domain, the RLS can be formulated as

$$\hat{\tilde{\mathbf{x}}} = \arg\min_{\tilde{\mathbf{x}}}\{\|\tilde{\mathbf{H}}\tilde{\mathbf{x}} - \tilde{\mathbf{y}}\|^2 + \lambda\|\tilde{\mathbf{x}}\|^2\}, \tag{7}$$

with the solution given by

$$\hat{\tilde{\mathbf{x}}} = (\tilde{\mathbf{H}}^T\tilde{\mathbf{H}} + \lambda\mathbf{I})^{-1}\tilde{\mathbf{H}}^T\tilde{\mathbf{y}}. \tag{8}$$

Multiresolution Representation of TLS

The TLS approach attempts to minimize the errors in both $\mathbf{y}$ and $\mathbf{H}$, i.e.,

$$\textit{minimize} \quad \|\,\Delta\mathbf{H}|\Delta\mathbf{y}\,\|_F\,, \tag{9}$$

$$\textit{subject to}\ (\mathbf{H} + \Delta\mathbf{H})\mathbf{x} = \mathbf{y} + \Delta\mathbf{y}. \tag{10}$$

Here $\|\cdot\|_F$ denotes the Frobenius norm. It has been shown that the constrained minimization problem in Eqs.(9-10) is equivalent to the minimization problem [6]

$$Minimize \quad \left\{ F(\mathbf{q}) = \frac{\mathbf{q}^T \mathbf{A}^T \mathbf{A} \mathbf{q}}{\mathbf{q}^T \mathbf{q}} \right\}, \qquad (11)$$

where $F(\mathbf{q})$ is called the Rayleigh quotient. Using wavelet multiresolution representation, one can formulate the TLS in the WT domain. Let

$$\tilde{\mathbf{A}} = [\tilde{\mathbf{H}} | \tilde{\mathbf{y}}], \quad \text{and} \quad \tilde{\mathbf{q}} = \begin{pmatrix} \tilde{\mathbf{x}} \\ -1 \end{pmatrix}. \qquad (12)$$

Then it can be shown easily that minimizing the Rayleigh quotient function defined in (11) is equivalent to the following problem:

$$Minimize \quad \left\{ F(\tilde{\mathbf{q}}) = \frac{\tilde{\mathbf{q}}^T \tilde{\mathbf{A}}^T \tilde{\mathbf{A}} \tilde{\mathbf{q}}}{\tilde{\mathbf{q}}^T \tilde{\mathbf{q}}} \right\}. \qquad (13)$$

That is, the TLS solution to the original equation (1) is equivalent to the TLS solution to the transform equation (4).

Multigrid Reconstruction Algorithm

We see from the previous section that wavelet decomposition of a signal leads to a multiresolution representation of the signal. If we exploit the multiresolution property, the computational time may be reduced. The idea of a two grid reconstruction algorithm is as follows: In the first (coarse) grid, we reconstruct the low-resolution subsignal, by assuming the detail signals are zero. Then in the next (fine) grid, we reconstruct the entire signal, starting from the solution obtained by interpolating the coarse solution.

In this paper, we employ a modified V-cycle multigrid algorithm. Specifically, let L represent the level of wavelet decomposition, this modified V-cycle algorithm consists of the following steps:

1. Perform wavelet transform of $\mathbf{y}$ and $\mathbf{H}$ to obtain $\tilde{\mathbf{y}}_l$ and $\tilde{\mathbf{H}}_l$, $l = -1, -2, ..., -L$. Set $l = -L$.

2. Solve for the RLS solution $\tilde{\mathbf{x}}_l$ of the perturbation equation at the lth level, $\tilde{\mathbf{H}}_l \tilde{\mathbf{x}}_l = \tilde{\mathbf{y}}_l$, using the CGD algorithm; Or for TLS solution:

2'. Solve for the TLS solution $\tilde{\mathbf{q}}_l$ and hence $\tilde{\mathbf{x}}_l$ at the l^{th} level, by minimizing $F(\mathbf{q}_l) = \frac{\tilde{\mathbf{q}}_l^T \tilde{\mathbf{A}}_l^T \tilde{\mathbf{A}}_l \tilde{\mathbf{q}}_l}{\tilde{\mathbf{q}}_l^T \tilde{\mathbf{q}}_l}$ using the CG algorithm in [5].

3. Prolongate from $\tilde{\mathbf{x}}_l$ to $\tilde{\mathbf{x}}_{l+1}$ by padding zeros, i.e., $\tilde{\mathbf{x}}_{l+1} = [\tilde{\mathbf{x}}_l^T, \mathbf{0}^T]^T$.

4. Let $l = l + 1$, if $l = 0$ stop, otherwise, go back to Step 2.

In the methods of [7], the regularization parameter is fixed at different resolutions. In our scheme, the regularization parameter at different grids (resolutions) are varied. In the coarse resolution, the noise in quite weak compared to the signal, so we do not need to apply much regularization. When the resolution goes from coarse to fine, the regularization parameter is increased. This is because the noise is more pronounced in high frequencies.

Currently, we have only implemented a two-grid algorithm ($L = 1$). The coarse level representation $\tilde{\mathbf{x}}_{-1}$ consists of the top left quarter of the entire wavelet transform $\tilde{\mathbf{x}}$ of $\mathbf{x}$, which includes the coefficients representing low frequencies components in both horizontal and vertical directions. This yields the coarse level reconstruction $\tilde{\mathbf{x}}_{-1}$. Starting from this solution, we then solve all the components of $\tilde{\mathbf{x}}$ or selected ROIs.

Experimental Results

In our experiment, the length-4 Daubechies' wavelet [8] is used because it achieves a good tradeoff between computational precision and computational complexity. Figs. 1 and 2 show the simulation results with a test medium in which a $1.5cm$ diameter rod is placed at an off-center position with respect to the source and detector ring. The rod has a nonhomogeneous absorption distribution, following a sinusoidal pattern (one positive cycle only) whose maximum value for μ_a is $0.05cm^{-1}$ and $\mu_s = 10cm^{-1}$. The background medium has $\mu_a^b = 0.02cm^{-1}$ and $\mu_s^b = 10cm^{-1}$. A total of 16 sources and 16 detectors are evenly spread about the rod in a ring geometry having a diameter of 10 cm. The forward solution in this experiment is obtained by a multigrid finite difference solver described in [3]. In this experiment, for the RLS approach, the data are corrupted by white Gaussian noise with an average noise level of 10%. For the TLS approach, the data are corrupted by white Gaussian noise with an average noise level of 3.3%. The weights are also corrupted by white Gaussian noise with the same noise variance as that in the detector reading. The noise level in the weights is very low compared to the average signal level, only 0.01%. But because the weight function has a very large dynamic range, more than 40% of weights are actually corrupted by a noise level of above 10%.

The original medium is shown in Fig. 1(a). Its wavelet transform is given in Fig. 1(b). Similarly, the detector reading and its wavelet transform are

given in Figs. 1(c) and 1(d). The detector readings are ordered into a two dimensional array, with the first row corresponding to the detector readings for the source located on the line formed by the origin and the absorber. This is why the detector readings are strongest at the four corners of the two dimensional graph. Fig. 2 shows the reconstruction results of RLS (left column) and TLS (right column). From this figure, we can see that we can obtain quite accurate results from the coarse level reconstruction alone (see Figs. 2 (c) and (g)) in about 1/7 and 1/10 of the time of the one grid reconstruction using RLS and TLS, respectively. With additional processing in the fine grid, the two-grid algorithm obtains approximately the same images as the one-grid method in 1/2 and 3/4 of the computation time of the one-grid method with the RLS and TLS, respectively. As can be seen from Fig. 1(b), the energy of the original image is mostly contained in the low-low frequency band. In general, this type of smooth image can be reconstructed very efficiently with the wavelet based multigrid method. Figs. 1(e) and 1(f) present the wavelet transforms of the reconstructed images using two grid RLS and TLS shown in Figs. 2(e) and 2(f), respectively.

Conclusion and Discussion

In this paper, a wavelet-based multiresolution reconstruction scheme is applied to obtain both RLS and TLS solutions of the perturbation equation. Compared to the one-grid method, we have demonstrated that the proposed method can produce images of comparable quality and accuracy at much lower computation costs. We have also shown that incorporation of regularization in the wavelet domain can effectively suppress image degradation caused by added noise. The incorporation of regularization terms to improve the stability of TLS solution remains a topic of our future study.

The wavelet based multigrid algorithm allows one to focus on special ROIs when going from coarse grid to fine grid. Further study is required for automatic detection of ROIs from coarse solutions.

Acknowledgement

This work was supported in part by the National Institutes of Health under Grant # RO1-CA59955, by an ONR grant # N000149510063, and by the New York State Science and Technology Foundation.

References

1. Y. Wang, J. Chang, R. Aronson, R.L. Barbour, H.L. Graber, and J. Lubowsky, "Imaging scattering media by diffusion tomography: An iterative perturbation approach," in *Proc. SPIE*, vol. 1641, pp. 58–71, Jan. 1992, Los Angeles.

2. J. Chang, Y. Wang, R. Aronson, H. L. Graber, and R.L. Barbour, "A layer stripping approach for recovery of scattering media from time-resolved data," in *Proc. SPIE*, vol. 1767, pp. 384–395, July 1992, San Dieg.

3. Y. Q. Yao, Y. Wang, Y. L. Pei, W. Zhu, J. H. Hu and R. L. Barbour, " Frequency Domain Optical Tomography In Human Tissue," in *Proc. SPIE* , vol. 2570, July, 1995, San Diego.

4. W. Zhu, Y. Wang, H. L. Graber, R. L. Barbour and J. Chang, "A Regularized Progressive Expansion Algorithm for Recovery of Scattering Media from Time-Resolved Data," in *Proc. of OSA Topical Meeting on Advances in Optical Imaging and Photon Migration* , pp.211-216, March, 1994, Orlando.

5. W. Zhu, Y. Wang, J. Chang, H. L. Graber, and R. Barbour, "A Total Least Squares approach for the solution of the perturbation equation," in *Proc. SPIE*, vol. 2398, pp.420-430, Feb. 1995, San Jose.

6. G. H. Golub, "Some Modified Matrix eigenvalue problems," *SIAM Review*, vol. 15, no. 2, pp. 318-334, April, 1973.

7. G. Wang, J. Zhang and G. W. Pan, "Solution of inverse problems in image processing by wavelet expansion," *IEEE Trans. on Image Processing*, vol. 4, no. 5, pp. 579-593, 1995.

8. C. K. Chui, An Introduction to Wavelets, Academic Press, 1991.

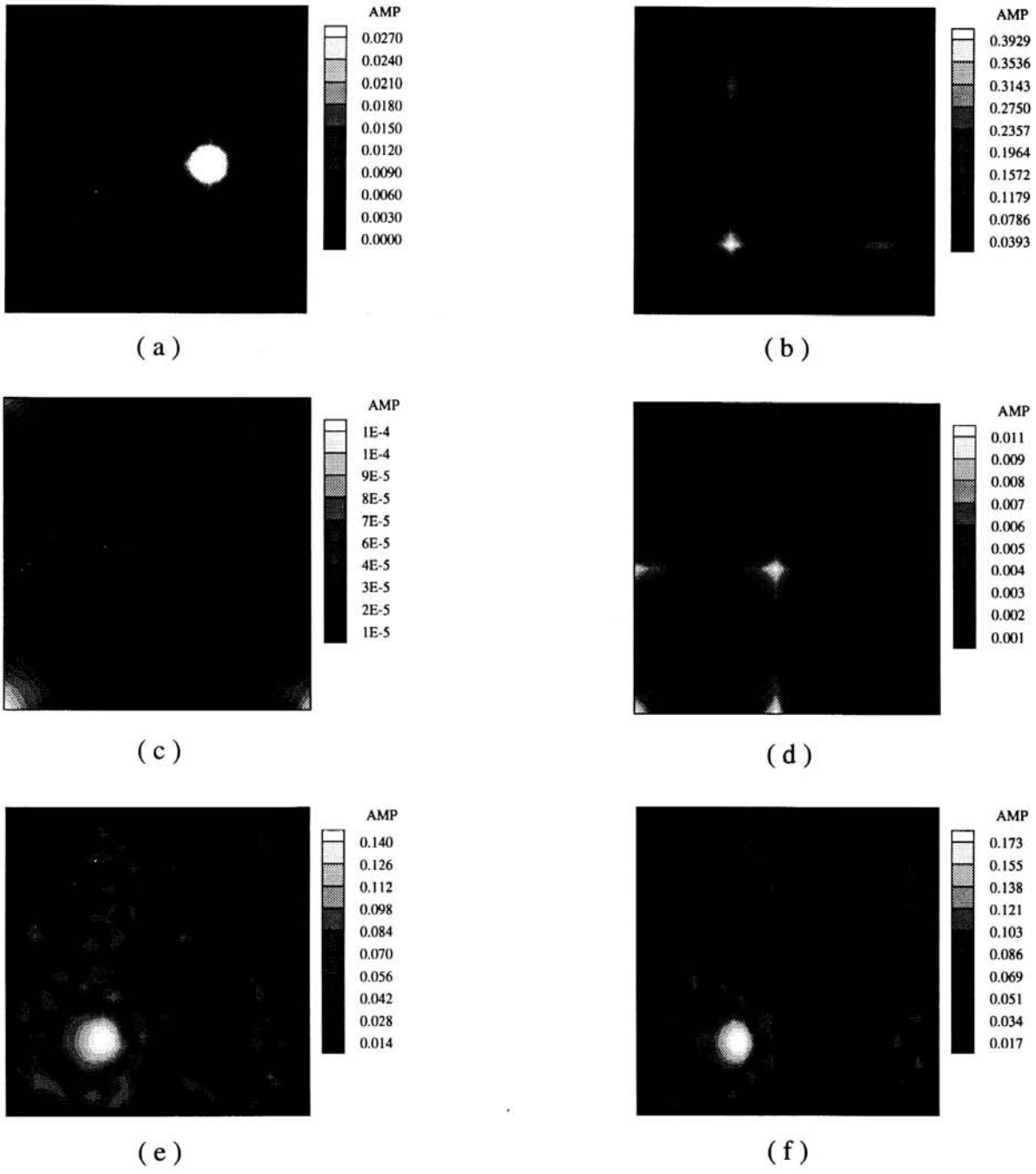

Figure 1: (a) The true image of the test medium; (b) the wavelet transform of (a); (c) the 2-D plot of detector readings; (d) the wavelet transform of (c); (e) the wavelet transform of reconstructed image by RLS, shown in Fig. 2(d); (f) the wavelet transform of reconstructed image by TLS, shown in Fig. 2(h). When plotting wavelet transform images (Figs. (b), (d), (e) and (f)), in order to reveal the high frequency subsignals, we have applied a "square-root" mapping to the signal magnitude.

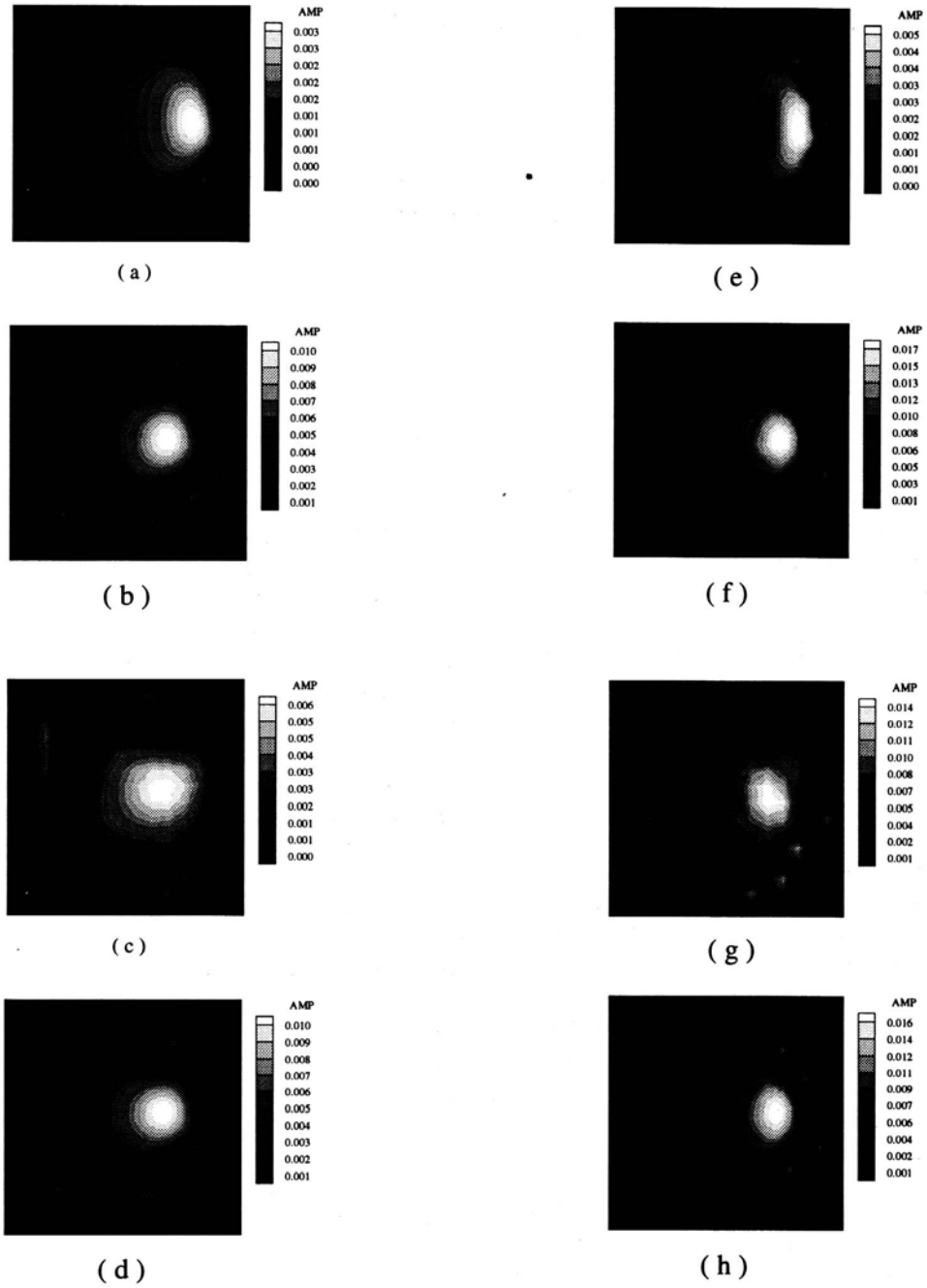

Figure 2: Reconstruction results of RLS (left column) and TLS (right column). (a) and (d) are obtained with the one-grid RLS method after 32 and 225 iterations, respectively; (c) and (d) are obtained with the two-grid RLS method after 500 iterations in the coarse grid and additional 100 iterations in the fine grid, respectively; (e) and (f) are obtained with the one-grid TLS method after 85 and 885 iterations, respectively; (g) and (h) are obtained with the two-grid TLS method after 1200 iterations in the coarse grid and additional 600 iterations in the fine grid, respectively. The computation time for (a) and (c), (e) and (g) are roughly the same, respectively; the time for (d) is about 1/2 of (b); the time for (h) is about 3/4 of (f). The time for (c) is about 1/7 of (b) and the time for (g) is about 1/10 of (f).